 https://doi.org/10.3311/PPci.22216

Periodica Polytechnica Civil Engineering, 68(3), pp. 912–924, 2024

Stiffness of Loaded Face of Steel Rectangular Hollow Section Columns with and without Concrete Infill in Beam-column Endplate Connections

Said Hicham Boukhalkhal[1,2], Abd Nacer Touati Ihaddoudène[1], Luis Filipe Da Costa Neves[3], Messaoud Saidani[4*]

[1] Built Environment laboratory LBE, Civil Engineering faculty, University of Sciences and Technology Houari Boumediene, Bab Ezzouar 16111, Algeria
[2] Laboratory of Mechanics and Materials Development, Department of Civil Engineering, University of Djelfa BP 3117, Djelfa, Algeria
[3] INESC, Civil Engineering Department, University of Coimbra, Rua Sílvio Lima, Pólo II, 3030-790 - Coimbra, Portugal
[4] Faculty of Engineering, Environment and Computing, School of Energy, Construction and Environment, Coventry University, Priory Street, Coventry CV1 5FB, UK
* Corresponding author, e-mail: cbx086@coventry.ac.uk

Received: 17 March 2023, Accepted: 16 February 2024, Published online: 13 May 2024

Abstract

This paper presents a new analytical approach for calculating the stiffness of the loaded face of a rectangular hollow section RHS column in beam-column connections with and without concrete infill, as well as with flush and extended endplates, to determine the behavior curve of these types of connections. The approach, based on Eurocode 03's component method, offers efficient analytical formulas for accurately determining the loaded face's stiffness. A comparison with existing methods demonstrates its remarkable simplicity and efficiency, allowing a simple beam model to represent the RHS column's behavior with all relevant parameters considered. Comparison of the new approach to existing ones from the literature demonstrates their reliability and efficiency. Furthermore, when compared to 32 experimental tests presenting nearly the entire range of probable connection configurations, as well as attachment techniques commonly used in construction practice, the margin of error does not exceed 12 percent on average and a maximum of less than 25 percent.

Keywords

Rectangular Hollow Section, column, stiffness, concrete infill, connections, analytical

1 Introduction

The use of hollow section columns in steel structures offers several structural and economic benefits. As an example, consider the increase in load-bearing capacity, particularly in concrete filled steel tube (CFST) columns. Furthermore, when compared to I- or H-profiles, hollow sections columns have equal strength in all directions, a significant decrease in structural weight and, as a result, a decrease in construction cost, a significant increase in fire resistance, and ease of implementation and maintenance during and after structure realization.

In practice, it is difficult to connect structural hollow sections with standard bolts and nuts because it is normally impossible to access the inside of the section to screw in the bolts [1].

Several studies have presented solutions for connecting I- or H-sections to hollow section columns. Among these studies [1–6], the CIDECT [7] has collaborated on research and development projects with the manufacturers of these systems. The FLOWDRILL drilling technique, Lindapter Hollo-Bolts, and welded studs are the most commonly used techniques for this type of connection.

The deformation or strength of the hollow section face, rather than that of the individual bolt, will often control the joint capacity in most connections that incorporate multiple bolts loaded in tension, as research works on I/H beam connections with hollow or concrete-filled columns (RHS, CHS) have demonstrated over the last few decades [7].

Cite this article as: Boukhalkhal, S. H., Ihaddoudène, A. N. T., Neves, L. F. D. C., Saidani, M. "Stiffness of Loaded Face of Steel Rectangular Hollow Section Columns with and without Concrete Infill in Beam-column Endplate Connections", Periodica Polytechnica Civil Engineering, 68(3), pp. 912–924, 2024. https://doi.org/10.3311/PPci.22216

Previous researchers have investigated the behavior of this type of connection and its impact on the overall response of the structure [8, 9]. The aim is to provide an approach that accounts for the deformation of the loaded face of the RHS column under different loads [10–16]. This study is motivated by the lack of formulas in existing standards that address this issue, AISC [8] and EC3 [17].

To evaluate the behavior of these types of connections, experimental, numerical, and analytical proposals are available [11, 13–15, 18], based on previously established classical theories and methods [19–21].

Ghobarah et al. [13] presented a method based on the calculation of three main parameters: endplate in bending, tube face deformation in the tension, and deformation of tube lateral face. The approach is semi-analytical as all of the formulas are related to numerical or experimental parameters, making it difficult to evaluate all the possible situations and configurations for this type of connection.

Neves [12] proposed a beam model for calculating the stiffness of the loaded tube face, and another plate model for calculating the effective length or the length that affects the inertia of the proposed beam. The formula for calculating the deformation of the tensioned column face is then derived, but only in the case of concrete-filled columns. This model is based on three key parameters: bolt diameter-to-tube width ratio; distance between bolt axes in a horizontal direction to tube width ratio; thickness to tube width ratio (slenderness). The results from the model are compared to experimental tests conducted on connections with extended or flush endplates. The limitation lies in its ratio, which directly affects the effective length l_{eff} and thus influences the stiffness of the tube face. It is also limited in connections involving several rows of bolts in the vertical direction. Even when using profiles with large cross-sections, it generates poor results due to the intersection of the effective lengths considered.

Park and Wang [10] calculated the stiffness of the tube face using Timoshenko's plate deformation theory with assumptions to simplify it [22]. Park and Wang's formula [10] can be applied to three different types of connections. Connections from a beam to a hollow column, a beam to a CFST column, and a beam to a *I* or *H* column in the minor axis. They created a powerful analytical equation to calculate the lateral deformation of the tube k_r, with errors of less than 10% when compared to experimental tests. In CFST columns, the stiffness tends to infinity, but in hollow columns, Park and Wang [10] proposed a long and complicated equation, which is therefore unsuitable for engineering practice. Additionally, investigation of the results of this approach shows that the tube face deformation equation gives acceptable results in connections with thin tube thickness because this approach is based on the plate theory. On the other hand, it underperforms in connections where the bolt diameter and tube thickness are important.

The approach proposed by Thai and Brian [14] uses a computer tool to evaluate the deformation of the column face in both hollow and concrete-filled steel tubes. It is based on numerical simulations, with empirical formulas developed to estimate tube deformation at each joint face. There are two types of joints used, and the connections can be unilateral or bilateral. In some connection configurations, these formulas produce incomprehensible results.

Existing approaches do not explicitly investigate the relationship between bolt diameter and tube thickness. This relationship has an immediate impact on the stiffness and failure mode of the connection. In the case of large bolt diameters, Maquoi et al. [23] and Korol et al. [9] demonstrated that the mode of failure of I-beam type connections with hollow RHS columns is through the loaded side of the column. However, as the diameter of the bolts decreases, the failure mode is generated by the bolts themselves. The parameter controlling the tube thickness and bolt diameter will be included in the calculations in the current study, and equations will be developed to demonstrate its influence on the initial stiffness of the connections. This geometrical parameter is denoted by ξ, which is the ratio of the bolt diameter to the RHS column thickness. It has a significant effect on the stiffness of the RHS column's face.

Furthermore, and in the context of studying the behavior of this type of connection in a way that introduces all the parameters that influence the connection stiffness, the current study also deals with the influence of the lateral face of the RHS hollow column, which was already proposed by Park and Wang [10]. The expression of such terms is also included in the equations developed.

The objective of this study is to demonstrate the possibility of addressing this problem using the component method adopted by EC3 [17] by adding new components indicating the deformability of the column face in RHS beam-column connections in both the hollow and concrete-filled cases. Analytical equations are used to calculate these components. They were validated and calibrated through experimental and numerical studies, which are available in the literature.

2 Component method

The component method used by EC3 and its Annex J [17] is based on the philosophy of isolating the connection

component and studying the linear behavior of each one using elastic springs, then reassembling according to the case studied to evaluate the overall behavior of the connection figures.

The main parameters calculated by this method are the initial stiffness, the moment of resistance, and rotation capacity, in order to obtain the moment-rotation curve, which represents the overall connection behavior.

The characteristics of the components [15] can be calculated using Annex J of EC3, such as endplate and flange angles in bending, beam flange in compression, beam web in tension, beam flange subjected to diametral pressure, and bolts in tension. However, in the case of the beam to hollow column connections, EC3 lacks these characteristics.

The purpose of this research is to create simple and effective analytical formulae that characterize the following components:

- Hollow column face in tension $k_{RHS,t}$ Fig. 1;
- Concrete filled column face in tension $k_{CFHS,t}$ Fig. 2;
- Hollow column face in compression $k_{RHS,c}$ Fig. 1.

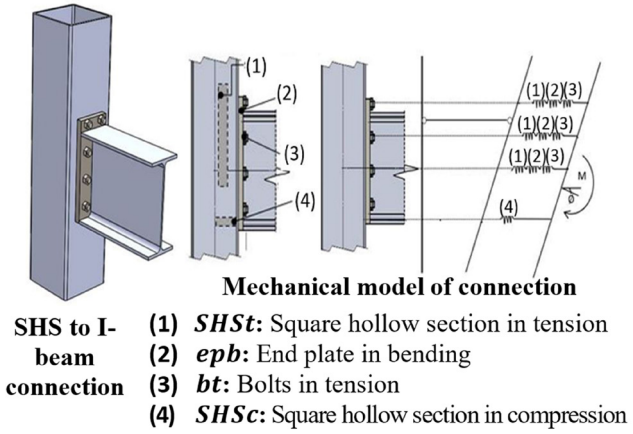

Fig. 1 Model for rigidity calculation of the hollow column without concrete

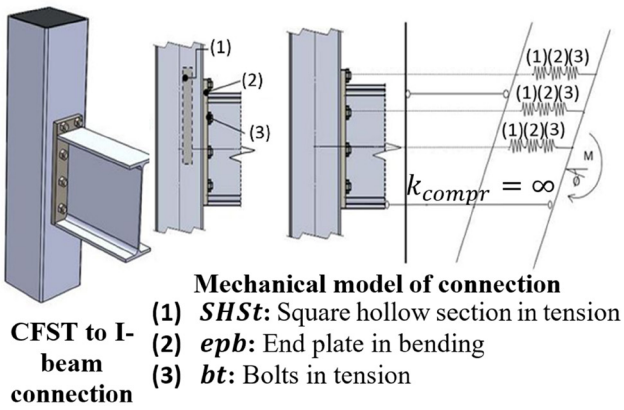

Fig. 2 Model for rigidity calculation of the hollow column with concrete

3 Proposed approach

In order to develop equations that evaluate the behavior of the RHS hollow column face in different stress zones (in tension and compression) and in both possible hollow or concrete-filled cases, an approach has been proposed based on the work of Costa-Neves [12] with modifications to simplify the problem and obtain simple equations that can be used in engineering practice.

The equivalent beam considered for this study is represented in Fig. 3. It is characterized by a moment of inertia I_{eff} Fig. 3 similar to that of Costa-Neves [12], as well as by the replacement of effective length I_{eff} by a new parameter called ξ that takes into account the effect of the bolt diameter and tube thickness in the calculations. Moreover, the stiffness coefficient k_r of Eq. (1) [10] takes into account the deformation of the lateral face of the tube, which is characterized by rotating springs at the ends of the equivalent beam, as shown in Figs. 4–6, with:

$$k_r = \begin{cases} \dfrac{4EI}{d_{\text{RHS}}}\left(\dfrac{1.5w_{\text{RHS}} + d_{\text{RHS}}}{2w_{\text{RHS}} + d_{\text{RHS}}}\right) \text{for RHS columns} \\ \dfrac{2EI}{B} \text{for open section in minor - axis} \end{cases} \quad (1)$$

Where: b, a, d_{RHS}, w_{RHS}, and k_r are respectively the bolt center distance in the horizontal direction, the effective

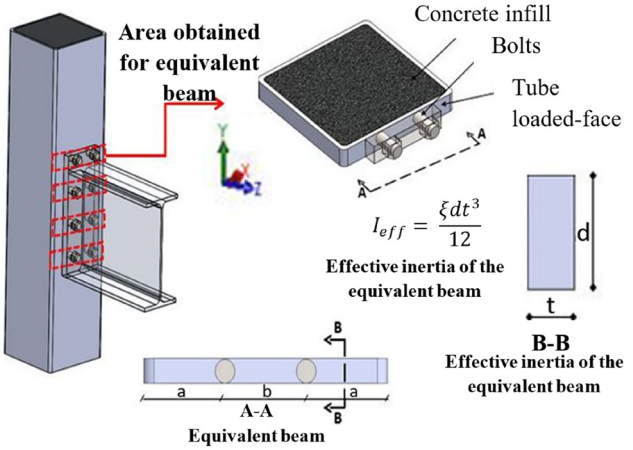

Fig. 3 Presentation of the proposed approach's modelling

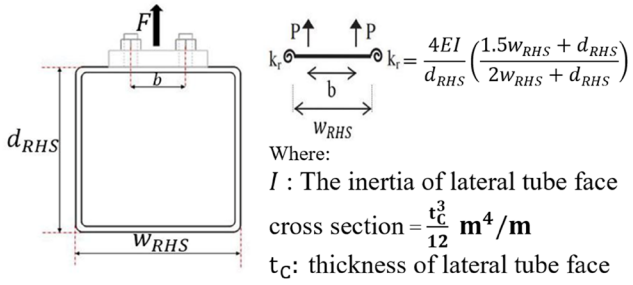

Fig. 4 Simplified connection model [10]

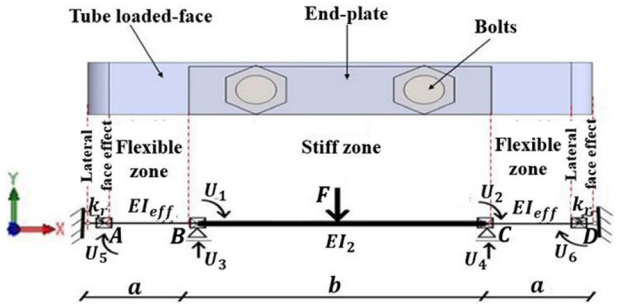

Fig. 5 Modelling of the equivalent beam in the tension zone

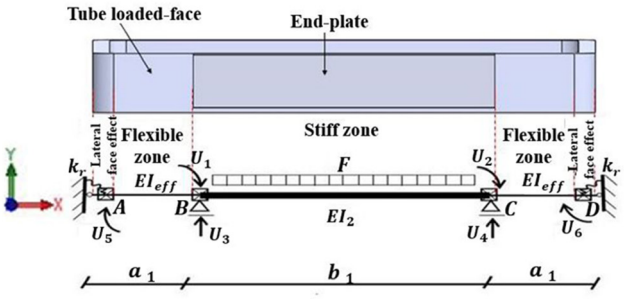

Fig. 6 Modelling of the equivalent beam in the compression zone

tube width, the lateral tube face length, the tube width and the stiffness of the lateral face of the tube as shown in Fig. 4.

3.1 Formulation

3.1.1 Stiffness of a hollow column's tensioned face without concrete

The equivalent beam model used to calculate the stiffness of the RHS column tensioned face is shown in Fig. 5. It is comprised of two inertia elements, I_{eff} and I_2, which represent the effective inertia that directly influences the deformation of the column face, and the infinitely rigid inertia that represents the other components of the connection, such as the plate and the I-beam.

The model is divided into three elements with different boundary conditions. In Fig. 5, A and D are represented by rotation spring k_r representing the stiffness of the lateral column face RHS as shown in Eq. (1). Supports B and C represented restricted rotations and allow only translation.

The global stiffness matrix of the equivalent beam is:

$$[K] = E \cdot \begin{bmatrix} 4\left(\frac{I_{eff}}{a}+\frac{I_2}{b}\right) & 2\frac{I_2}{b} & 6\left(\frac{I_{eff}}{a^2}-\frac{I_2}{b^2}\right) & 6\frac{I_2}{b^2} & 2\frac{I_{eff}}{a} & 0 \\ 2\frac{I_2}{b} & 4\left(\frac{I_{eff}}{a}+\frac{I_2}{b}\right) & -6\frac{I_2}{b^2} & -6\left(\frac{I_{eff}}{a^2}-\frac{I_2}{b^2}\right) & 0 & 2\frac{I_{eff}}{a} \\ 6\left(\frac{I_{eff}}{a^2}-\frac{I_2}{b^2}\right) & -6\frac{I_2}{b^2} & 12\left(\frac{I_{eff}}{a^3}-\frac{I_2}{b^3}\right) & -12\frac{I_2}{b^3} & 6\frac{I_{eff}}{a^2} & 0 \\ 6\frac{I_2}{b^2} & -6\left(\frac{I_{eff}}{a^2}-\frac{I_2}{b^2}\right) & -12\frac{I_2}{b^3} & 12\left(\frac{I_{eff}}{a^3}+\frac{I_2}{b^3}\right) & 0 & -6\frac{I_{eff}}{a^2} \\ 2\frac{I_{eff}}{a} & 0 & 6\frac{I_{eff}}{a^2} & 0 & 4\frac{I_{eff}}{a}+\frac{k_r}{E} & 0 \\ 0 & 2\frac{I_{eff}}{a} & 0 & -6\frac{I_{eff}}{a^2} & 0 & 4\frac{I_{eff}}{a}+\frac{k_r}{E} \end{bmatrix} \quad (2)$$

The vector of forces is given by:

$$\{F\} = \frac{F}{2}\left\{\frac{-b}{4} \quad \frac{b}{4} \quad 1 \quad 1 \quad 0 \quad 0\right\} \quad (3)$$

The equilibrium equation of the system is:

$$\{F\} = [K] \cdot \{U\} \quad (4)$$

After solving the system of equations, the displacement vectors are:

$$\begin{cases} U_1 = -U_2 = 0 \\ U_3 = U_4 = -\dfrac{Fa^3\left(4EI_{eff}+ak_r\right)}{24EI_{eff}\left(EI_{eff}+ak_r\right)} \\ U_5 = -U_6 = \dfrac{Fa^2}{4\left(EI_{eff}+ak_r\right)} \end{cases} \quad (5)$$

U_3 and U_4 represent the deformation of the tube face when the effect of the RHS column's lateral face stiffness is taken into account. The bending stiffness of the RHS column tensioned face without concrete is given by the expressions Eq. (6).

$$S_j = \frac{24EI_{eff}\left(EI_{eff}+ak_r\right)}{a^3\left(4EI_{eff}+ak_r\right)} \quad (6)$$

and

$$I_{eff} = \frac{\xi dt^3}{12}, \quad (7)$$

where, ξ: the proposed geometric ratio equal to d / t to account for the effect of bolts. It is calibrated and specified

numerically in the next paragraph. *d*: the diameter of the bolts. *t*: the column face thickness.

$$a = \frac{L-b}{2} \tag{8}$$

with, *a*: the distance between the tube edge and the bolts, *L*: the width of RHS column face, *E*: Young's modulus, *b*: the width of the tensioned area of the column face is equal to $b = b_0 + 0.9d$ according to Gomes et al. 1994 [18, 24] as shown in Fig. 7, where b_0 is the distance between bolt axes in the horizontal direction of connection, Fig. 3.

To simplify the calculations, geometric parameters *B*, *D*, and *T* are adopted. They are distinguished by the ratio of the width of the tensioned or compressed zone, the diameter of the bolts, the thickness of the column face, and the width of the stressed column face, in that order. They are given as follows:

$$\begin{cases} B = \dfrac{b}{L} \\ D = \dfrac{d}{L} \\ T = \dfrac{t}{L} \end{cases} \tag{9}$$

By replacing Eqs. (1), (7), (8) and (9) in (6), the bending stiffness of the tensioned face of the hollow column without concrete is given as:

$$S_{\mathrm{RHS},t} = \frac{16E\psi\xi T^3 L}{\left(1-B\right)^3} \tag{10}$$

With $\psi = \dfrac{\left(10BT+9B-18T-15\right)}{\left(10BT+9B-42T-33\right)}$.

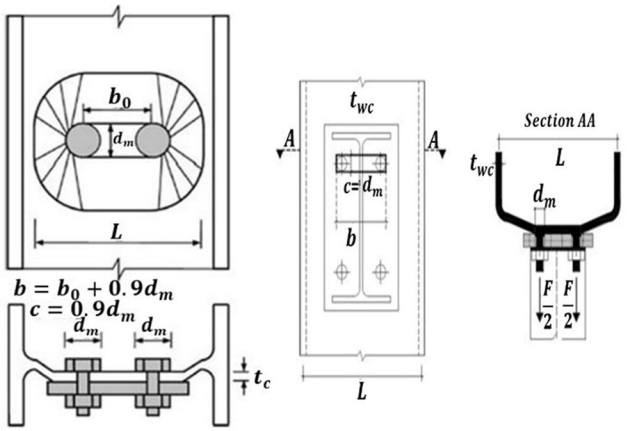

Fig. 7 Gomes model for the weak axis of the joint [18]

3.1.2 Stiffness of a concrete-filled hollow column's tensioned face

When concrete-filled columns are used, the lateral stiffness k_r of the column may be assumed equal to infinity because the concrete body prevents almost all deformations except the tensioned face [10, 11, 13]. In this case, Eq. (6) becomes:

$$S_j = \frac{24EI_{eff}}{a^3} \tag{11}$$

By substituting by the appropriate values, the flexural stiffness of the tensioned face of CFST column is:

$$S_{CFHS,t} = \frac{16E\xi DT^3 L}{\left(1-B\right)^3} \tag{12}$$

3.1.3 Stiffness of a hollow column's compressed face

Because the influence of the connection represented by the endplate and the bolts is influenced differently in the tensioned area, the area and intensity of loading will change in this case.

Fig. 6 represents a new representation of the equivalent beam in the compressed area of the column where the load becomes distributed, resulting in the force vector becoming as follows:

$$\left\{F\right\} = \frac{F}{2}\left\{\frac{-b_1^2}{6} \quad \frac{b_1^2}{6} \quad b_1 \quad b_1 \quad 0 \quad 0\right\} \tag{13}$$

The loading area will also change as follows:

$$a_1 = 2t \tag{14}$$

After solving the system of equations, the flexural rigidity is:

$$S_j = \frac{24EI_{eff}\left(EI_{eff}+k_r a_1\right)}{a_1^3 b_1\left(4EI_{eff}+k_r a_1\right)} \tag{15}$$

Substituting Eqs. (1), (7), (9), (14) into Eq. (15), the following flexural stiffness of the compressed face of the hollow column without concrete is obtained:

$$S_{\mathrm{RHS},c} = \frac{E\xi D\left(0.16+1.05T\right)L}{2.5+4.2T} \tag{16}$$

3.2 Initial stiffness of joints

The component method is used to calculate the initial stiffness of beam to hollow column connections with/without concrete infills, with the addition of new components characterizing the loaded face of RHS column in tension and compression. Table 1, Figs. 1, and 2 summarize the

Table 1 Steps of calculating the initial stiffness. $S_{j,ini}$

Component	Formula
Bolts in tension $k_{10,indv}$ (mm)	$1.6A_s / l_b$
Endplate in bending $k_{5,indv}$ (mm)	$0.9l_{eff}t_p^3 / m^3$
Hollow column face in tension $k_{RHS,t}$ (mm)	$\frac{16\psi\xi T^3 L}{(1-B)^3}$
Concrete filled column face in tension $k_{CFHS,t}$ (mm)	$\frac{16\xi DT^3 L}{(1-B)^3}$
Hollow column face in compression $k_{RHS,c}$ (mm)	$\frac{\xi D(0.16+1.05T)L}{2.5+4.2T}$
Equivalent stiffness for one row of bolts k_{eq} (mm)	$\sum k_{indv}h_r / z_{eq}$
Lever arms z_{eq} (mm)	$\frac{\sum k_{eff}h_r^2}{\sum k_{eff}h_r}$
Initial stiffness of the joint $S_{j,ini}$ (kN m/rad)	$\frac{Ez^2}{\sum k_{eq}}$

steps to calculating the initial stiffness. Where A_s, l_b, l_{eff}, t_p and m are bolt strength area, bolts length, effective length of T-stub flange, thickness of the end-plate and geometrical dimensions characterizing the position of the potential yield line in the T-stub flange, respectively. For more details, see Table 6.11 of EC3 part 1–8 [17].

3.3 Moment resistance of joints

The moment resistance of the connection is calculated by the following formula adopted from EC3 [17]:

$$M_{Rd} = \sum F_{bi} z_i \tag{17}$$

Where represents the plastic strength corresponding to the row of bolt "i". The strength of each row of bolt is the minimum of the strengths of the hollow column face F_{RHSi}, the tensioned bolts F_{10i} and the endplate in bending F_{5i}. The formulae for each strength are given in Annex J of EC3 except the strength of the hollow column face.

The model used by Gomes [18], shown in Fig. 7, for calculating the strength of connections in the minor axis is used in this study. The steps to follow are:

$$F_{RHS\ i} = M_{pl} k \eta \tag{18}$$

where,

$$\begin{cases} M_{pl} = 0.25 f_y t^2 \\ k = \begin{cases} 1 & si(\alpha+\beta) > 0.5 \\ 0.7+0.6(\alpha+\beta) & si(\alpha+\beta) \le 0.5 \end{cases} \\ \eta = \frac{4}{1-\beta}\left(\pi\sqrt{1-\beta}+2\alpha\right) \\ \alpha = \frac{c}{L}, \beta = \frac{b}{L} \end{cases} \tag{19}$$

Where, α: Bolt diameter to tube width ratio, β: Distance between the bolt axes in the horizontal direction to the width of the tube ratio, M_{pl}: Plastic moment and f_y: Elastic limit.

3.4 Moment-rotation curve of connection

The relationship between the moment and the relative rotation of the joint is used to describe the non-linear behavior of semi-rigid joints such as the bolted end-plate joint. Richard et al. [25] proposed that the moment-rotation relationship be represented by four parameters, as shown in Fig. 8. The model is represented by the following Eq. [25]:

$$M = \frac{(R_0 - R_p)\theta}{\left(1+\left|\frac{(R_0-R_p)\theta}{M_0}\right|^{\gamma}\right)^{\frac{1}{\gamma}}} + R_p\theta \tag{20}$$

where M is the moment of the joint, θ is the relative rotation between the elements of the joint, R_0 is the initial stiffness, R_p is the plastic stiffness, M_0 is the reference moment, and γ is the shape parameter of the curve.

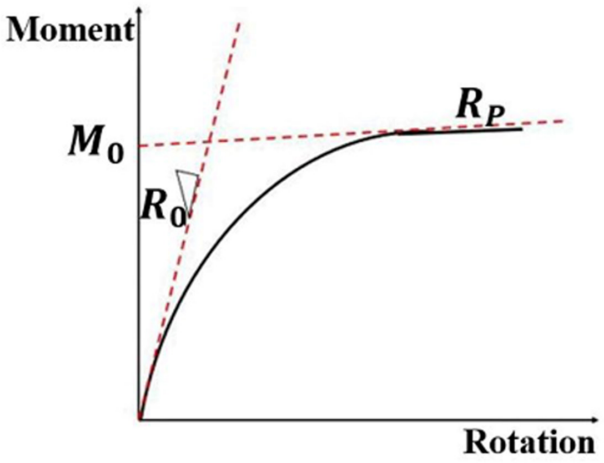

Fig. 8 Richard-Abbott model of the semi-rigid connection [25]

4 Numerical study

A numerical study was performed using the ANSYS software [26] to demonstrate the effect of bolt diameter to RHS tube thickness ratio on the initial stiffness of the CFST column face.

The numerical model used in this study is depicted in Figs. 9–11. It is made of a square steel tube of dimensions 200 × 200 mm, with a height of four times its width in order to limit the effects of boundary conditions [14].

The finite element model employed in this study utilizes SOLID187 [26], a 3D 10-Node Structural Solid element with ten nodes and three degrees of freedom each (translation in x, y, and z directions). The model utilizes the Homogeneous Structural Solid variant, suitable for general 3D solid structures and allowing prism and tetrahedral options degeneration in irregular regions. Both steel and concrete materials can be represented in the model. Mesh convergence studies were conducted to obtain a suitable tetrahedral mesh, providing reliable results with reduced computational time.

Material behavior curves were defined for the columns in the model: bilinear elastic perfectly plastic with hardening for RHS columns and multi-linear elasticity for CFST columns. These characteristics were implemented using the ANSYS code [26], while the material and geometric properties were consistent with the experimental tests. For the mixed prototypes (steel-concrete), a surface-to-surface model was used to ensure appropriate force transfer between interacting surfaces. CONTA173 and CONTA174 served as contact elements, while TARGE170 acted as the target surface. The contact surfaces were assumed to exhibit friction with a coefficient of 0.2 [27].

Regarding loading, point forces excited the tensioned face of the hollow columns (with or without concrete), interacting with a rigid element represented by the bolt diameter face. In the compressed zone, the load was distributed over a rigid element to prevent rotation and account for geometric effects and material inelasticity with large deflection.

The columns were assumed fixed at both ends, and this constraint was reflected in the finite element model by restraining the translation in all directions of a portion of the Square Hollow Section front face ($U_x = U_y = U_z = 0$).

The analysis is composed of three columns. Variants used according to their thickness (200 × 200 × 6, 200 × 200 × 8, 200 × 200 × 10) with a variation relating to the bolt diameter. In each case, the loading zone changes according to the bolt diameter used. The different situations studied are summarized in Table 2.

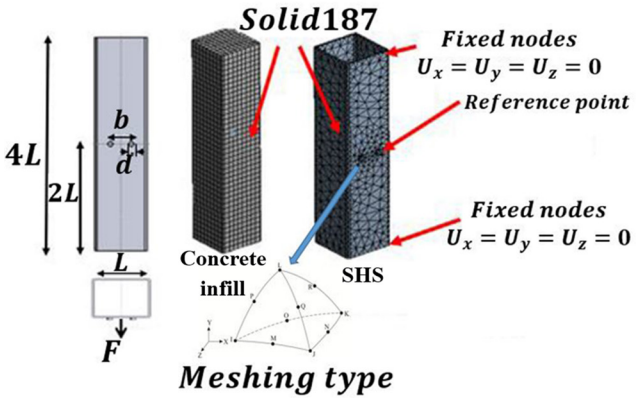

Fig. 9 Numerical model of CFST column's tensed area

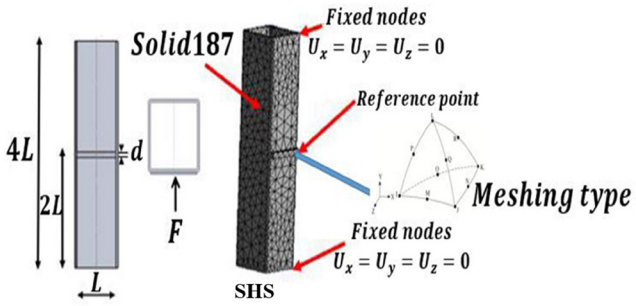

Fig. 10 Numerical model of SHS column's compressed area

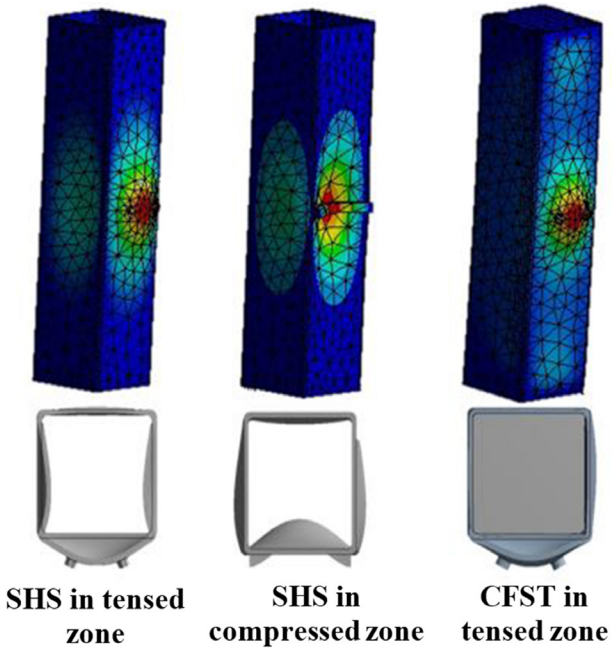

Fig. 11 Elements meshing and deformed shape of the prototypes studied

Table 2 The different situations studied of RHS columns

Test	d = 16 mm			d = 20 mm			d = 22 mm			d = 24 mm		
	B	D	T	B	D	T	B	D	T	B	D	T
T1	0.42	0.08	31.3	0.42	0.09	31.3	0.42	0.10	31.3	0.42	0.11	31.3
T2	0.43	0.08	23	0.43	0.09	23	0.43	0.10	23	0.43	0.11	23
T3	0.44	0.08	18	0.44	0.10	18	0.44	0.11	18	0.44	0.12	18

T1, T2 and T3 represent the columns 200X200X6, 200X200X8 and 200X200X10. d is the bolt diameter.

4.1 Validation of the numerical model

A comparison between the numerical model results and those obtained from the experimental tests of Costa-Neves et al. [12] and France et al. [28] was undertaken to validate the numerical model developed. Under the same material, geometry, and loading conditions, the force-displacement curves of both experimental and numerical models are shown in Fig. 12. The comparison demonstrates the reliability of the numerical model and its agreement with the experimental results.

4.2 Simulation results

A non-linear static analysis was performed to calculate the displacements on the column face without and with concrete infill. The results obtained are compared with the proposed formulas to calibrate the geometric coefficient ξ for each case. Tables 3–5 compare the initial stiffness of the numerical model and the proposed analytical approach for each of the three situations, T1, T2, and T3.

The results of the numerical model and the analytical approach proposed in the framework of evaluating the stiffness of the tensioned or compressed face of the column in the two mentioned cases (hollow or concrete filled) show that the geometrical parameter ξ is explicitly influence the stiffness of the loaded face of the RHS column.

4.3 Comparison with existing approaches

Figs. 13–15 compare the values of the proposed stiffness of the loaded face of the CFST column $k_{CFHS,t}$ to those obtained using the Costa-Neves [12] and Thai and Brian [13] approaches.

Since both approaches are based on the same beam model, the stiffness curves for the proposed and Costa-Neves approaches are nearly identical if $L / t = 30$. If, on the other hand, the ratio is void, the deviation tends to increase.

On the other hand, the curves show that if the ratio d / L changes, the results from the two approaches are identical, especially for low values of B.

The application of tensile forces in the case of the proposed approach and that of Thai and Brian [16], as well

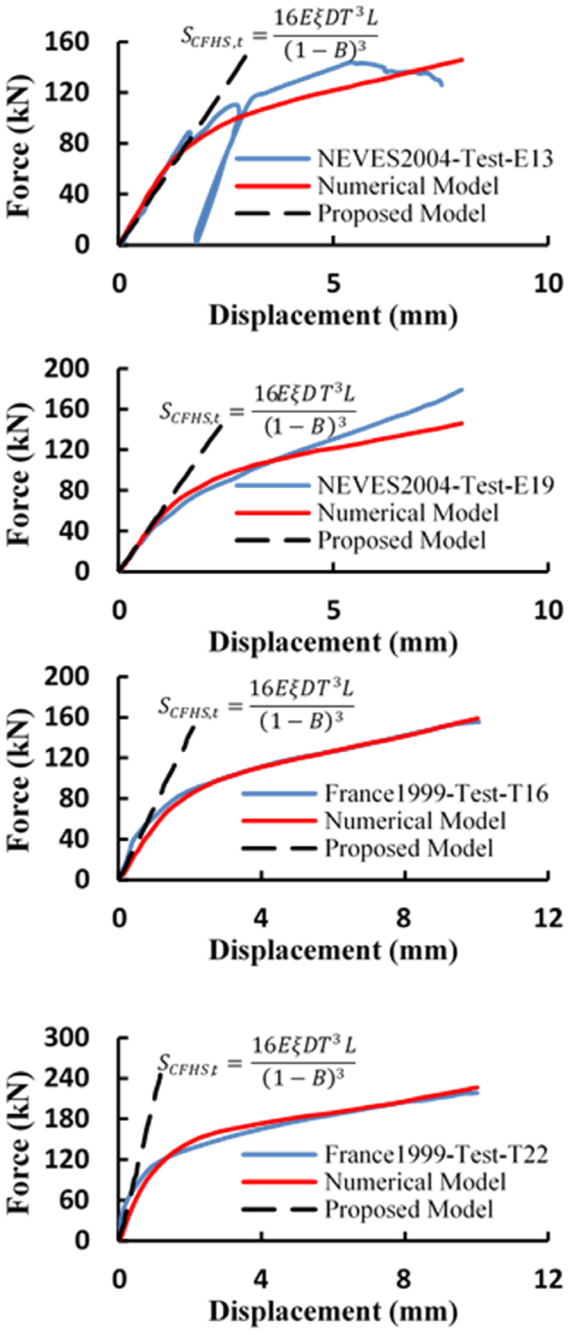

Fig. 12 Comparison of experimental tests from [12] and [28] versus the numerical model results, for tests E13, E19, T16 and T22

Table 3 Initial stiffness of the numerical model and the proposed analytical approach (T1)

CASE	$S_{j,num}$	$S_{j,ana}$	$\xi_{ana} = d/t$	$\xi_{num} = S_{j,num} / S_{j,ana}$	ξ_{ana} / ξ_{num}
T1-D16	26 891	10 871.63	2.67	2.47	0.93
T1-D20	54 124	15 080.10	3.33	3.59	1.08
T1-D22	65 634	17 498.18	3.67	3.75	1.02
T1-D24	78 593	20 155.75	4.00	3.90	0.97

Table 4 Initial stiffness of the numerical model and the proposed analytical approach (T2)

CASE	$S_{j,num}$	$S_{j,ana}$	$\xi_{ana} = d/t$	$\xi_{num} = S_{j,num} / S_{j,ana}$	ξ_{ana} / ξ_{num}
T2-D16	73 913	31 555.00	2.00	2.34	1.17
T2-D20	86 734	32 422.00	2.50	2.68	1.07
T2-D22	123 697	37 620.73	2.75	3.29	1.20
T2-D24	132 302	43 334.67	3.00	3.05	1.02

Table 5 Initial stiffness of the numerical model and the proposed analytical approach (T3)

CASE	$S_{j,num}$	$S_{j,ana}$	$\xi_{ana} = d/t$	$\xi_{num} = S_{j,num} / S_{j,ana}$	ξ_{ana} / ξ_{num}
T3-D16	115 158	57 066.25	1.60	2.02	1.26
T3-D20	116 700	63 324.00	2.00	1.84	0.92
T3-D22	118 430	66 798.18	2.20	1.77	0.81
T3-D24	206 564	84 637.92	2.40	2.44	1.02

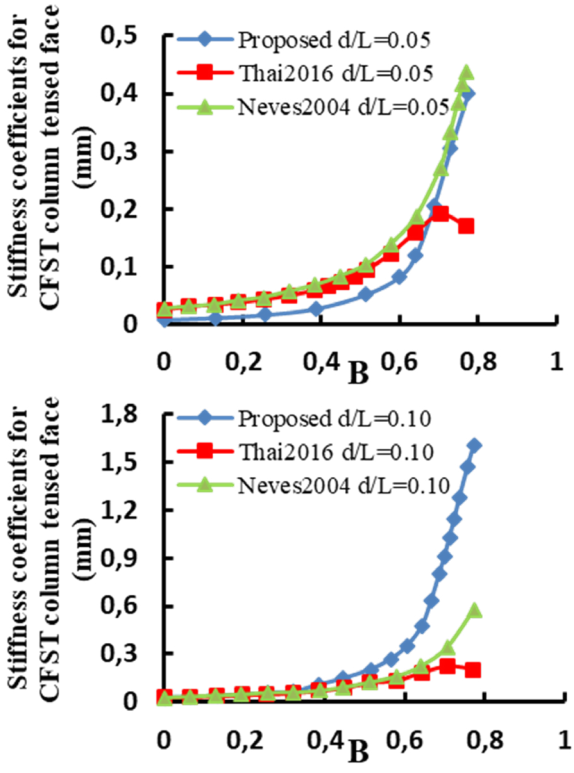

Fig. 13 Stiffness coefficientscompared with current approaches for L/t = 50

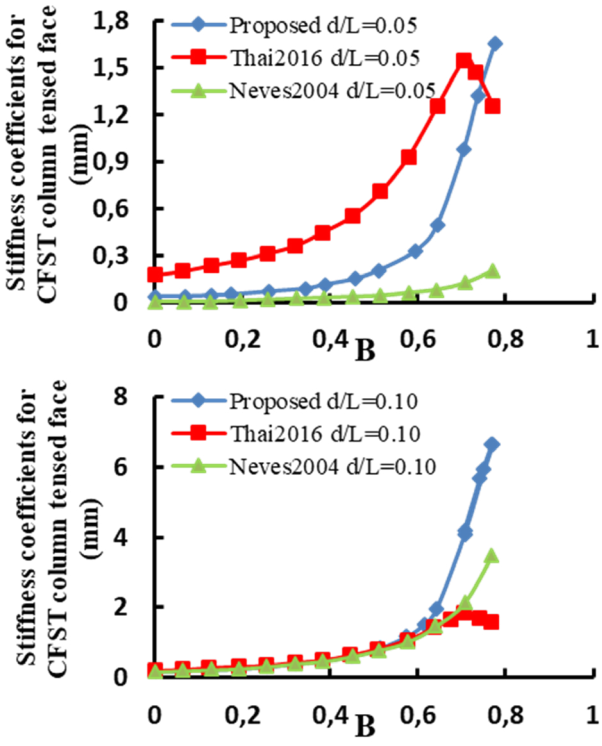

Fig. 14 Stiffness coefficientscompared with current approaches for L/T = 30

as the consideration of the influence of the bolt diameter on the tube thickness, explain the reason for the variation between the compared approaches.

Furthermore, the current model exhibits underestimation for small values of D and overestimation for large values of B in most scenarios involving slenderness (L / t).

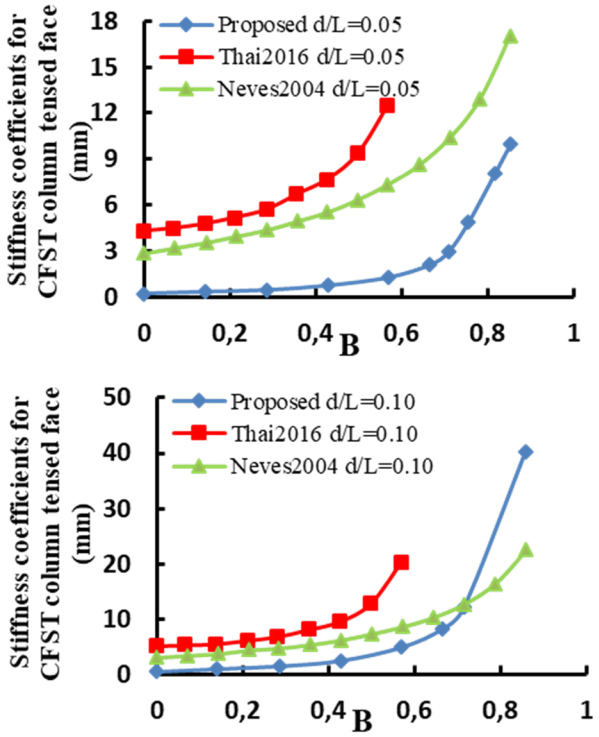

Fig. 15 Stiffness coefficientscompared with current approaches for L/t = 10

This disparity with other established methods can be attributed to two primary factors: firstly, the proposed model accounts for the influence of bolts diameter in the initial stiffness; secondly, the two alternative approaches rely on plate theory, where shear forces effects are nearly insignificant, while the proposed model adopts beam theory, giving importance to shear and consequently providing more precise results in comparison to experimental tests, as detailed in the subsequent paragraph of this paper.

5 Validation with experimental tests

A comparison with the experimental results with regards the initial stiffness and the joint's behavior curve ($M - \phi$) was performed as part of the validation of the proposed approach.

France et al. [28–30] conducted a series of 20 experimental tests on beam-column connections with extended and flush endplates, as well as RHS columns with and without concrete infill. The Flowdrill technique was used to connect the beam to the hollow column. References [28–30] detail the configurations of all the connections used. Comparison can be made with 17 tests in this study.

The method of components is used to calculate the initial stiffness $S_{j,ini}$ of the connection. Table 6 compares the

Table 6 Comparison of the initial analytical stiffness with the tests of France et al. [28–30]

	End-plate type	Conc / filling	$S_{j,ini}$ (kN m / rad) Experimental	$S_{j,ini}$ (kNm / rad) Proposed	Error (%)	$S_{j,ini}$ (kN m / rad) Park and Wang [10]	Error (%)
T2	Flush	-	12 500.00	11 045.88	11.63	14 358.00	−14.86
T4	Flush	-	5 800.00	5 454.87	5.95	4 942.00	5.00
T5	Flush	-	3 700.00	3 404.70	7.98	4 179.00	−12.95
T6	Flush	-	9 000.00	8 735.60	2.94	5 793.00	6.60
T7	Flush	-	3 200.00	3 757.61	−17.43	2 173.00	−2.50
T8	Flush	-	13 000.00	9 853.88	24.20	26 227.00	−14.00
T10	Flush	-	1 960.00	1 668.24	14.89	1 648.00	15.92
T18	Flush	-	5 350.00	5 729.36	−7.09	5 417.00	−1.25
T19	Flush	-	31 000.00	26 239.87	15.36	25 793.00	16.80
T20	Extended	-	60 000.00	56 349.94	6.08	53 873.00	10.21
T21	Extended	-	68 000.00	54 241.16	20.23	146 478.00	−17.20
T23	Extended	-	65 000.00	55 741.74	14.24	55 392.00	14.78
T14	Flush	Yes	33 300.00	31 432.62	5.61	26 019.00	21.86
T15	Flush	Yes	18 600.00	15 293.44	17.78	10 141.00	45.48
T16	Flush	Yes	16 000.00	15 579.95	2.63	4 697.00	70.64
T17	Flush	Yes	3 810.00	4 279.23	−12.32	4 492.00	−17.90
T22	Extended	Yes	120 000.00	131 416.71	−9.51	104 185.00	13.18
T24	Extended	Yes	120 000.00	135 153.67	−12.63	104 119.00	13.23
				Average	11.58		17.46
				Max	24.20		70.64

experimental results with those obtained using the analytical method. Stiffnessis $S_{j,ini}$ calculated using both the Park and Wang approach [10] and that proposed.

The proposed approach, as shown in Table 6, has an average margin of error of 11.58 percent with a maximum margin of no more than 24.20 percent, whereas the Park and Wang approach [10] has an average margin of 17.46 percent with a maximum margin of 70.64 percent. The values are compared based on the France et al. [28–30] results. Park and Wang [10] calculated the initial stiffness from different points than those used by France et al. [28–30]. These findings indicate that the proposed method is appropriate for use in such contexts. Furthermore, they demonstrate that using plate theory to evaluate column face deformation is not appropriate in some cases where the column thickness and/or end plate are important.

Comparison with Costa-Neves [12] tests on beam-to-CFST-column connections attached by welded studs is shown in the Table 7. Similar to the results of the comparison with France et al. [28–30] tests, the margin of error is small on average, equal to 7.41 percent, which is acceptable in construction practice.

Furthermore, a comparison of the analytical results of the new approach and the one developed by Costa-Neves [12] reveals that replacing the geometrical coefficient instead of the effective length improved the results and increased the model's margin of use, particularly in connections composed of several rows of bolts and sizable profile sections.

In terms of the $(M-\phi)$ curves, the results show that using the non-linear Richard-Abbott model [25] in beam-to-RHS hollow column connections with/without concrete infills is appropriate and safe, i.e., giving conservative curves retains some safety in the design Fig. 16. Similar to these findings, a comparison of the new approach and the one developed by Ghobarah et al. [13] yielded the same conclusions Fig. 16, particularly in the elastic phase, but the plastic stiffness is approximated in the post-elastic phase. It is always dependent on the designer's appropriate performance, the experimental results, and the material class used.

Another verification will be performed using the HolloBolts attachment technique, used by Tizani et al. [16]. The comparison results are shown in Table 8. The margin of error is 4 percent, indicating that the new approach seems to have little effect on the change in the attachment technique.

Table 7 Comparison of the initial analytical stiffness with the tests of Costa-Neves [12]

	Endplate type	Concrete filling	$S_{j,ini}$ kN m / rad Experimental	$S_{j,ini}$ kN m / rad Proposed	Error (%)	$S_{j,ini}$ kN m / rad Costa-Neves [12]	Error (%)
E13	Extended	Yes	4 323.00	4 486.85	−3.79	4 768.40	−10.30
E14	Extended	Yes	2 687.00	2 432.00	9.49	2 582.00	3.91
E16	Extended	Yes	7 051.00	6 799.60	3.57	7 177.00	−1.79
E17	Extended	Yes	3 027.00	2 871.18	5.15	3 923.00	−29.60
E19	Flush	Yes	2 015.00	1 711.84	15.05	1 801.30	10.61
				Average	7.41		11.24
				Max	15.05		29.60

Table 8 Comparison of the initial analytical stiffness with the tests of Tizani et al. [16]

	Endplate type	Concrete filling	$S_{j,ini}$ (kN m / rad) Experimental	$S_{j,ini}$ (kN m / rad) Proposed	Erreur (%)
T1	Flush	Yes	45 000.00	43 280.34	3.82
T2	Flush	Yes	56 000.00	55 372.05	1.12
T3	Extended	Yes	75 000.00	69 888.69	6.82
T4	Flush	Yes	40 400.00	38 478.81	4.76
T5	Flush	Yes	22 000.00	21 707.83	1.33
T6	Flush	Yes	82 500.00	76 713.71	7.01
T7	Flush	Yes	32 500.00	31 238.88	3.88
				Average	4.11
				Max	7.01

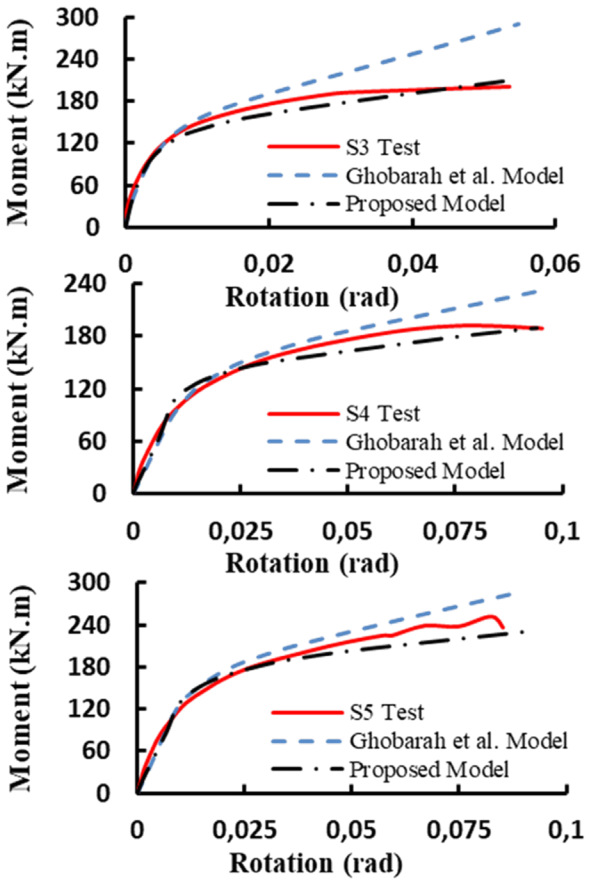

Fig. 16 Comparison of the proposed approach's (M-ϕ) curve with the tests of Ghobarah et al. [13]

6 Conclusions

This paper presents a simplified method for calculating the stiffness of the RHS hollow column face without or filled with concrete in beam-to-RHS column connections with an endplate. The comparison between this newly proposed method and existing approaches highlights its remarkable simplicity and efficiency. Unlike other methods, this approach allows for the utilization of a simple beam model to accurately represent the behavior of the RHS column's face while considering all the relevant parameters influencing the connection's behavior. Moreover, the proposed method's validity is substantiated through a comprehensive comparison with 32 experimental tests encompassing a wide range of configurations and attachment techniques commonly employed in construction practice. Remarkably, the proposed method exhibits an average margin of error of no more than 12%, with a maximum deviation of 25%. The ability to achieve highly accurate results with a minimal margin of error is a significant advantage, making this method a valuable addition to the existing approaches used in structural engineering and construction design. Furthermore, by incorporating the component method from Eurocode 03 [17], the proposed approach aligns itself with established standards, ensuring compatibility with prevailing design practices. The analytical formulas developed through this research enable engineers to streamline the calculation process while obtaining precise results, ultimately leading to more efficient and cost-effective structural designs. Overall, this paper offers a comprehensive and innovative contribution to the field of structural engineering, providing a simplified yet accurate means of determining the stiffness of beam-to-RHS column connections. The potential implications of this method extend to various construction projects, offering engineers a reliable tool to optimize and enhance the performance of their designs while maintaining safety and compliance with industry standards.

References

[1] Boukhalkhal, S. H., Ihaddoudène, A. N. T., Costa-Neves, L. F., Madi, W., Vellasco, P. C. G., Lima, L. "Numerical modelling of CFST column to I beam end plate joints", ce/papers – Proceedings in Civil Engineering, 4(2–4), pp. 989–994, 2021. https://doi.org/10.1002/cepa.1388

[2] Serrano-López, M. A., López-Colina, C., Wang, Y. C., Lozano, M., García, I., Gayarre, F. L. "An experimental study of I beam-RHS column demountable joints with welded studs", Journal of Constructional Steel Research, 182, 106651, 2021. https://doi.org/10.1016/j.jcsr.2021.106651

[3] García, I., Serrano, M. A., López-Colina C., Gayarre, F. L. "The stiffness of beam-to-RHS joints with welded studs", Journal of Building Engineering, 70, 106340, 2023. https://doi.org/10.1016/j.jobe.2023.106340

[4] Barros, H. T. G., Oliviera, M. M., Sarmanho, A. M. C., Alves, V. N. "Stiffness assessment of welded I-beam to RHS column connections", Engineering Structures, 267, 114661, 2022. https://doi.org/10.1016/j.engstruct.2022.114661

[5] Xu, X., Cheng, R., Yang, P., Chen, K., Li, J. "Behavior of T-shaped CFST column and U-shaped steel-concrete composite beam joints", Journal of Building Engineering, 43, 103157, 2021. https://doi.org/10.1016/j.jobe.2021.103157

[6] Li, B., Yang, Y., Liu, J., Liu, X., Cheng, Y., Chen, Y. F. "Behavior of T-shaped CFST column to steel beam connection with U-shaped diaphragm", Journal of Building Engineering, 43, 102518, 2021. https://doi.org/10.1016/j.jobe.2021.102518

[7] Kurobane, Y., Packer, A. J., Wardenier, J., Yeomans, N. "Guide de dimensionnement pour les assemblages de poteaux structurels en profil creux" (Sizing guide for structural column connections in hollow sections), TÜV Media, 2006. ISBN 978-3824909735 (in French)

[8] CSI "Steel Frame Design Manual AISC 360-05/IBC 2006 For ETABS 2016", Computer & Structures, Inc., USA, 2016. [online] Available at: https://usermanual.wiki/Document/SFDAISC36005.3738151137/view

[9] Korol RM, Ghobarah A, Mourad S. "Blind Bolting W-Shape Beams to HSS Columns", Journal of Structural Engineering, 119(12), pp. 3463–3481, 1993. https://doi.org/10.1061/(asce)0733-9445(1993)119:12(3463)

[10] Park, A. Y., Wang, Y. C. "Development of component stiffness equations for bolted connections to RHS columns", Journal of Constructional Steel Research, 70, pp. 137–152, 2012. https://doi.org/10.1016/j.jcsr.2011.08.004

[11] Costa-Neves, L., Silva, L. S., Vellasco, P. C. G. S. "A Model for Predicting the Stiffness of Beam to Concrete Filled Column and Minor Axis Joints under Static Monotonic Loading", In: Eurosteel 2005: 4th European conference on steel and composite structures, Maastricht, Netherlands, 2005, pp. 131–138. ISBN 3861308126

[12] Costa-Neves, L. "Monotonic and cyclic behaviour of minor-axis and tubular joints in steel and steel and concrete composite structures", PhD thesis, University of Coimbra, 2004.

[13] Ghobarah A., Mourad, S., Korol, R. M. "Moment-rotation relationship of blind bolted connections for HSS columns", Journal of Constructional Steel Research, 40(1), pp. 63–91, 1996. https://doi.org/10.1016/S0143-974X(96)00044-2

[14] Thai, H.-T., Uy, B. "Rotational stiffness and moment resistance of bolted endplate joints with hollow or CFST columns", Journal of Constructional Steel Research, 126, pp. 139–152, 2016. https://doi.org/10.1016/j.jcsr.2016.07.005

[15] Vandegans, D. "Liaison entre poutres métalliques et colonnes en profils creux remplis de béton, basée sur la technique du goujonnage (goujons filetés)" (Connection between metal beams and columns in hollow profiles filled with concrete, based on the doweling technique (threaded studs), CRIF MT 193 Brussels, Belgium, 1995. (in French)

[16] Tizani, W., Al-Mughairi, A., Owen, J. S., Pitrakkos, T. "Rotational stiffness of a blind-bolted connection to concrete-filled tubes using modified Hollo-bolt", Journal of Constructional Steel Research, 80, pp. 317–331, 2013. https://doi.org/10.1016/j.jcsr.2012.09.024

[17] ECS "EN 1993-1-8. Eurocode 3: Design of Steel Structures Part 1.", European Comimittee for Standardization, Brussels, Belgium, 2005.

[18] Gomes, F., Jaspart, J. P., Maquoi, R. "Behaviour of Minor-Axis Joints and 3-D Joints", In: COST C1: Semi-rigid Behaviour of Civil Engineering Structural Connections. Proceedings of the Second State of the Art Workshop, Prague, Czech Republic, 1994, pp. 111–120. ISBN 9782872631377

[19] Costa-Neves, L., F. Gomes, F. "Semi-rigid behaviour of beam-to-column minor-axis joints", IABSE reports, 75, pp. 207–218, 1996. https://doi.org/10.5169/seals-56911

[20] Costa-Neves, L. F., Costa, C. S. S. R., Lima, L. R. O., Jordão, S. "Optimum design of steel and concrete composite building structures", Structures and Buildings, 167(11), pp. 678–690, 2014. https://doi.org/10.1680/stbu.13.00022

[21] Costa-Neves, L. F., Silva, J. G. S. S., Lima, L. R. O., Jordão, S. "Multi-storey multi-bay buildings with composite steel-deck floors under human-induced loads: The human comfort issue", Computers & Structures, 136, pp. 34–46, 2014. https://doi.org/10.1016/j.compstruc.2014.01.027

[22] Timoshenko, Sz. "Theory of plates and shells", McGraw-Hill Book Company, 1940.

[23] Maquoi, R., Naveau, X., Rondal, J. "Beam-column welded stud connections", Journal of Constructional Steel Research, 4(1), pp. 3–26, 1984. https://doi.org/10.1016/0143-974X(84)90032-4

[24] Gomes, F., Jaspart, J-P., Maquoi, R. "Moment capacity of beam-to-column minor-axis joints", IABSE reports, 75, pp. 319–326, 1996. https://doi.org/10.5169/seals-56922

[25] Richard, R. M., Abbott, B. J. "Versatile Elastic-Plastic Stress-Strain Formula", Journal of the Engineering Mechanics Division, 101(4), pp. 511–515, 1975. https://doi.org/10.1061/JMCEA3.0002047

[26] ANSYS "ANSYS Release 15.0. Finite element program system" [computer program] Available at: https://forum.ansys.com/forums/topic/ansys-15-student-version-download/

[27] Dai, X., Lam, D. "Numerical modelling of the axial compressive behaviour of short concrete-filled elliptical steel columns", Journal of Constructional Steel Research, 66(7), pp. 931–942, 2010. https://doi.org/10.1016/j.jcsr.2010.02.003

[28] France, J. E., Davison, J. B., Kirby, P. A. "Moment-capacity and rotational stiffness of endplate connections to concrete-filled tubular columns with Flowdrilled connectors", Journal of Constructional Steel Research, 50(1), pp. 35–48, 1999. https://doi.org/10.1016/S0143-974X(98)00237-5

[29] France, J. E., Davison, J. B., Kirby, P. A. "Strength and rotational response of moment connections to tubular columns using Flowdrill connectors", Journal of Constructional Steel Research, 50(1), pp. 1–14, 1999. https://doi.org/10.1016/S0143-974X(98)00235-1

[30] France, J. E., Davison, J. B., Kirby, P. A. "Strength and rotational stiffness of simple connections to tubular columns using flowdrill connectors", Journal of Constructional Steel Research, 50(1), pp. 15–34, 1999. https://doi.org/10.1016/S0143-974X(98)00236-3